Bioorganic & Medicinal Chemistry 22 (2014) 5692–5696

Contents lists available at ScienceDirect

Bioorganic & Medicinal Chemistry

journal homepage: www.elsevier.com/locate/bmc

In situ formation of H_2O_2 for P450 peroxygenases

Caroline E. Paul [a,†], Ekaterina Churakova [a,†], Elmer Maurits [a], Marco Girhard [b], Vlada B. Urlacher [b,*], Frank Hollmann [a,*]

[a] Department of Biotechnology, Delft University of Technology, Julianalaan 136, 2628 BL Delft, The Netherlands
[b] Institute of Biochemistry, Heinrich-Heine-Universität Düsseldorf, Universitätsstraße 1, 40225 Düsseldorf, Germany

ARTICLE INFO

Article history:
Received 18 April 2014
Revised 23 May 2014
Accepted 28 May 2014
Available online 11 June 2014

Keywords:
P450 peroxygenases
mNADHs
In situ H_2O_2 generation
Hydrogen peroxide shunt
Oxyfunctionalization

ABSTRACT

An in situ H_2O_2 generation approach to promote P450 peroxygenases catalysis was developed through the use of the nicotinamide cofactor analogue 1-benzyl-1,4-dihydronicotinamide (BNAH) and flavin mononucleotide (FMN). Final productivity could be enhanced due to higher enzyme stability at low H_2O_2 concentrations. The H_2O_2 generation represented the rate-limiting step, however it could be easily controlled by varying both FMN and BNAH concentrations. Further characterization can result in an optimized ratio of FMN/BNAH/O_2/biocatalyst enabling high reaction rates while minimizing H_2O_2-related inactivation of the enzyme.

1. Introduction

Synthetic nicotinamide cofactor analogues (mNADHs) such as 1-benzyl-1,4-dihydronicotinamide (BNAH, Scheme 1) were previously shown to be functional mimics of their natural, more complex counterparts.[1] For example, they have been demonstrated to promote alcohol dehydrogenase-catalyzed reduction reactions,[2–4] monooxygenase-catalyzed oxyfunctionalizations,[5,6] and, more recently, to be excellent substitutes for NAD(P)H in ene-reductase-mediated C=C-bond reductions.[7]

In the course of our ongoing efforts to exploit the synthetic potential of mNADHs for biocatalysis, we realized that the reactivity of, for example, BNAH towards free flavins exceeds the reactivity of their native counterparts by orders of magnitude. Combined with the high reactivity of reduced flavins towards molecular oxygen (yielding oxidized flavins and hydrogen peroxide),[8] this might be exploited as a convenient system for the catalytic in situ generation of H_2O_2 to promote peroxidase reactions (Scheme 2).

To test our hypothesis, we chose the cytochrome P450 peroxygenases $P450_{Bs\beta}$ (CYP152A1) from *Bacillus subtilis*[9] and $P450_{Cl\alpha}$ (CYP152A2) from *Clostridium acetobutylicum*.[10] $P450_{Bs\beta}$ and $P450_{Cl\alpha}$ catalyze the α- and β-hydroxylation of fatty acids thereby exhibiting an interesting chemical reactivity not found amongst chemical oxidation/oxyfunctionalisation catalysts. Furthermore, both enzymes were demonstrated to exhibit significant activity in the so-called hydrogen peroxide shunt pathway,[9–11] as does also $P450_{Sp\alpha}$ from *Sphingomonas paucimobilis*—the first characterized enzyme of the CYP152 subfamily.[12] That is, these enzymes are capable of forming the catalytically active ferric hydro-peroxy species directly from the resting state of the enzyme using H_2O_2 as oxidant. From a preparative point of view, this reactivity is highly interesting as it circumvents the need of an expensive nicotinamide cofactor together with a regeneration system, as well as the (likewise complicated) electron transport chain.[13–15] Unfortunately, heme-dependent enzymes are prone to fast inactivation in the presence of elevated H_2O_2 concentrations due to oxidative modification of the heme prosthetic group.[16] Therefore, stoichiometric addition of H_2O_2 has to be avoided. In recent years, several in situ H_2O_2 generation methods based on the reductive activation of molecular oxygen have been reported, amongst them, enzymatic,[17] chemical,[18] electrochemical [19–22] and photochemical systems.[11,23–25]

The aim of the present study was to evaluate the suitability of the proposed chemical, flavin-catalyzed in situ H_2O_2-generation system to promote $P450_{Cl\alpha}$ and $P450_{Bs\beta}$-catalyzed oxyfunctionalisation reactions.

2. Results and discussion

2.1. In situ generation of H_2O_2

In a first set of experiments, we evaluated the parameters influencing the H_2O_2-generation rate of the system BNAH/FMN/O_2.

* Corresponding authors. Tel.: +49 211 8113889 (V.B.U.), +31 15 2781957 (F.H.).
E-mail addresses: vlada.urlacher@hhu.de (V.B. Urlacher), f.hollmann@tudelft.nl (F. Hollmann).
† Both authors contributed equally.

http://dx.doi.org/10.1016/j.bmc.2014.05.074
0968-0896/

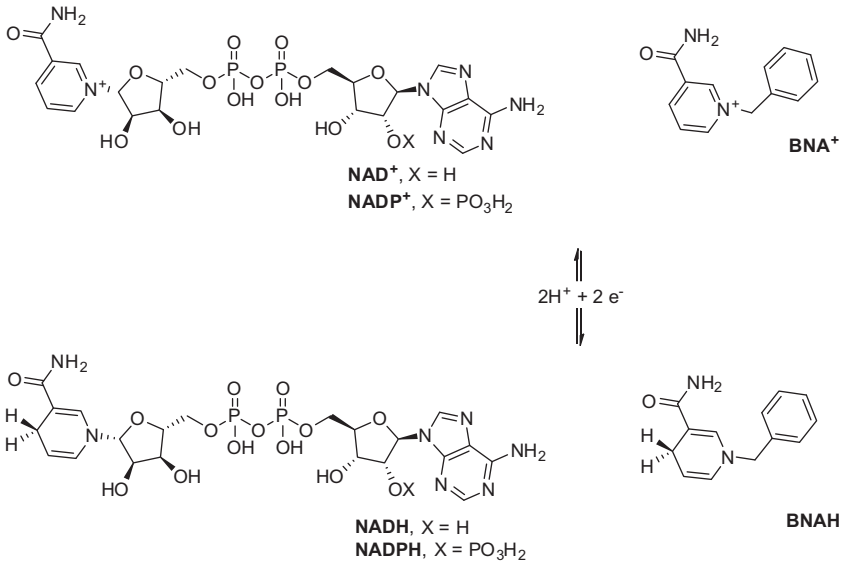

Scheme 1. Comparison of the structures and basic electrochemical features of natural nicotinamide cofactors and synthetic analogues such as BNA.

For this, we varied independently the concentrations of BNAH and FMN (Fig. 1). It is worth mentioning here that the reaction rate can be determined by either following the characteristic UV-absorption of BNAH (at 360 nm), or by following the concentration of dissolved oxygen, or by quantifying the amount of H_2O_2 formed. Within experimental error all methods gave the same results.

As shown in Figure 1, the initial reaction rate linearly depended on both, the concentration of BNAH and FMN. A significant deviation from linearity was observed only in the presence of very high concentrations of either component. Considering the rather high O_2-reduction rates, we assume that this deviation from linearity may be due to the poor solubility of O_2 in aqueous media (ca. 0.25 mM) and O_2-diffusion from the gas phase to the reaction mixture becoming overall rate-limiting.

Overall, we concluded that the BNAH/FMN/O_2 system allows for highly predictable and reproducible in situ generation of H_2O_2 necessary to promote P450-peroxygenase catalyzed oxyfunctionalizations.

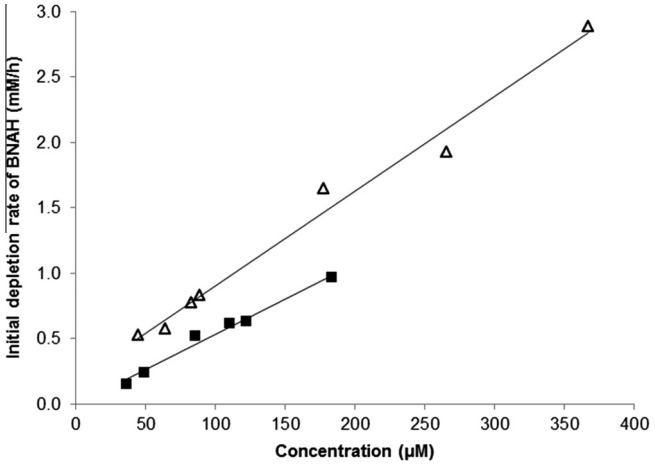

Figure 1. Initial depletion rate of BNAH with varying BNAH (Δ) concentration ([FMN] = 120 μM), and FMN (■) concentration ([BNAH] = 85 μM).

2.2. Enzymatic hydroxylation

Once the generation of H_2O_2 with BNAH and FMN was established, the process was applied for the hydroxylation of myristic acid **1** by the heme-containing peroxygenases $P450_{Cl\alpha}$ and $P450_{Bs\beta}$ to obtain the 2- and/or 3-hydroxymyristic acid products **2** and **3**, respectively (Scheme 1). The first experiments were performed under arbitrarily chosen conditions with cell-free extracts for 20 min. Pleasingly, the enzyme-catalyzed hydroxylation proceeded smoothly, leading to 75% and 95% conversion for $P450_{Cl\alpha}$

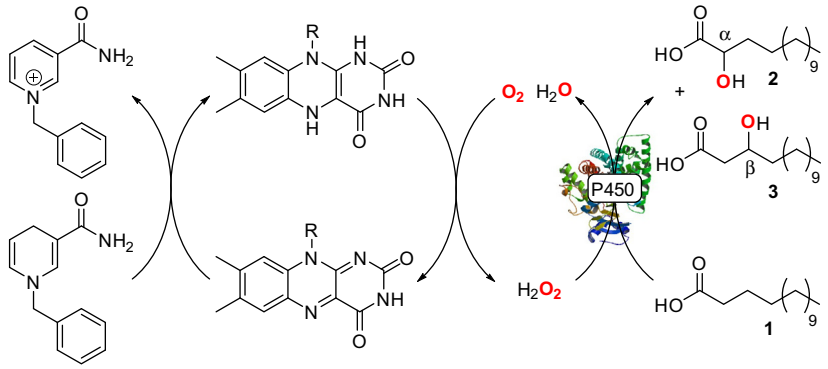

Scheme 2. Proposed chemoenzymatic system for the hydroxylation of fatty acids. BNAH is used as stoichiometric reductant reducing FMN (flavin adenine mononucleotide). The reduced FMN quickly reacts with molecular oxygen to yield H_2O_2 (hence FMN acts as transfer hydrogenation catalyst between BNAH and O_2). Finally, H_2O_2 regenerates the catalytically active ferric hydro-peroxy species in P450 peroxygenases (such as $P450_{Bs\beta}$ and $P450_{Cl\alpha}$) to perform selective hydroxylation of, for example, myristic acid.

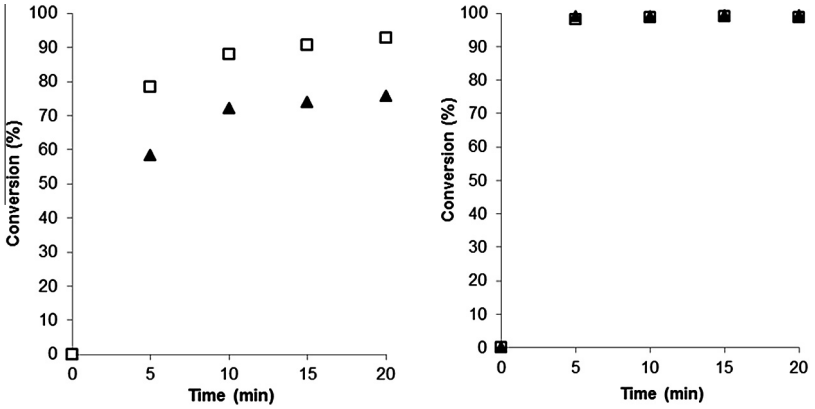

Figure 2. Hydroxylation time course of myristic acid with in situ H_2O_2 generation; $P450_{Cl\alpha}$ (▲), $P450_{Bs\beta}$ (□). Left: with cell-free extracts; right: with purified enzymes. Tris–HCl buffer (50 mM, pH 7.5), [myristic acid] = 200 μM, [BNAH] = 600 μM, [FMN] = 60 μM, [P450] = 1 μM, 30 °C.

and $P450_{Bs\beta}$, respectively (Fig. 2, left). The product distribution (α:β ratio of the hydroxylated products **2** and **3**) was 24:1 for $P450_{Cl\alpha}$ and 1:1.7 for $P450_{Bs\beta}$, respectively. These results are in good accordance with the product distributions observed previously and therefore appears to reflect the intrinsic selectivity of these enzymes.[9–11,26] It should be mentioned here that no other (by)products than the ones mentioned have been observed in all reactions.

Performing the same reactions with purified enzyme led to even higher product concentrations, achieving full conversion after only 5 min (Fig. 2, right). We attribute this apparent higher activity to the presence of endogenous catalases in the crude *Escherichia coli* cell extracts competing with $P450_{Cl\alpha}$ or $P450_{Bs\beta}$ for the H_2O_2 generated.

In the case of the purified enzymes, both exhibited identical activities (turnover frequency of 40 min^{-1}), which may indicate that the chemocatalytic H_2O_2 generation reaction is overall rate-limiting. In fact, with 40 min^{-1} the catalytic activities significantly fall back behind the rates observed with stoichiometric amounts of H_2O_2 being 200 and 1200 min^{-1} for $P450_{Cl\alpha}$ or $P450_{Bs\beta}$, respectively.[9,10] Under these conditions, however, rapid inactivation of the enzymes was also observed resulting in maximally 40% conversion of the starting material. Therefore, we conclude that the lower activity in our case is over-compensated by the higher robustness of the reaction scheme leading to overall higher productivities. Similar observations were made using photochemical in situ generation of H_2O_2.[11]

2.3. BNAH and FMN concentrations

Hoping to optimize the enzymes' performance by increasing the H_2O_2 generation rate, we systematically varied the concentrations of

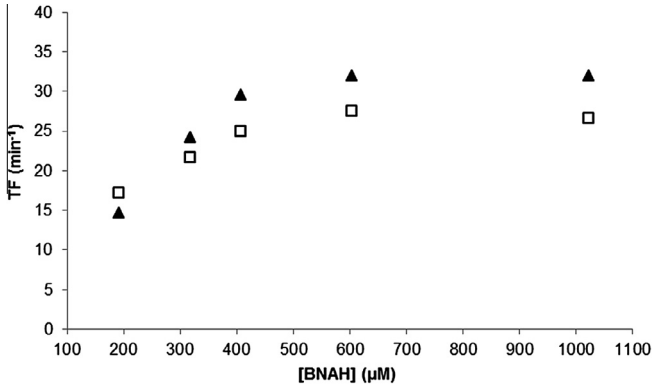

Figure 3. Turnover frequency (TF) with varying BNAH concentrations; $P450_{Cl\alpha}$ (▲), $P450_{Bs\beta}$ (□). Tris–HCl buffer (50 mM, pH 7.5), [myristic acid] = 200 μM, [FMN] = 60 μM, [P450] = 1 μM (cell-free extracts), 30 °C, 5 min.

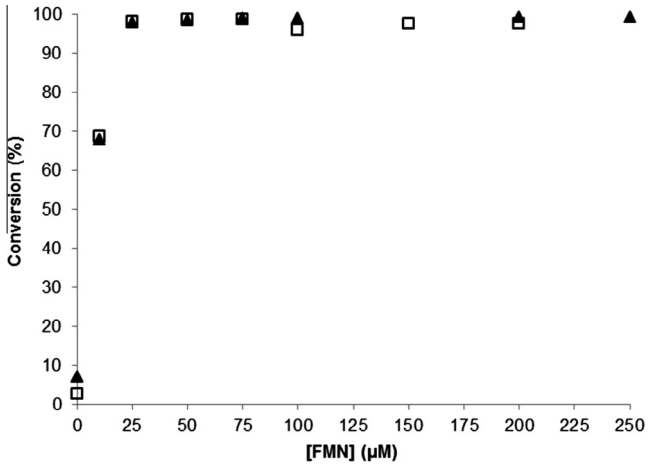

Figure 4. Product **2** and **3** formation with varying FMN concentrations; $P450_{Cl\alpha}$ (▲), $P450_{Bs\beta}$ (□). Tris–HCl buffer (50 mM, pH 7.5), [myristic acid] = 200 μM, [BNAH] = 600 μM, [P450] = 1 μM (purified enzyme), 30 °C, 5 min.

BNAH and FMN while keeping all other parameters constant (Figs. 3 and 4). Especially increasing the BNAH concentration had a significant influence on the overall reaction rate (Fig. 3). However, it should be mentioned here that these experiments were performed using crude cell extracts putatively containing endogenous *E. coli* catalases, resulting in an unproductive consumption of H_2O_2. Increasing the FMN concentration above 25 μM did not result in any significant increase of the overall reaction rate (Fig. 4). Interestingly enough, in both series a maximal activity of both, $P450_{Cl\alpha}$ and $P450_{Bs\beta}$ of ca. 35 min^{-1} was observed, corresponding to a product accumulation rate of ca. 2.1 mM h^{-1}. This corresponds well to the value under which in previous studies O_2 diffusion limitation has been suspected to become overall rate-limiting.[23]

We therefore expect that further studies optimizing the aeration of the reaction mixtures (or reducing the biocatalysts' concentrations) will yield higher activities for $P450_{Cl\alpha}$ and $P450_{Bs\beta}$.

2.4. Semi-preparative scale

Encouraged by the promising results of the process, a semi-preparative scale of the $P450_{Cl\alpha}$-catalyzed hydroxylation was carried out with 10 mM of myristic acid **1**. Despite the low solubility of both BNAH and myristic acid **1**, we avoided using co-solvents and performed the reaction as a suspension containing the aqueous mixture of the insoluble substrates. However, the reaction

yielded only 4% of the hydroxylated products **2** and **3** over a reaction period of 70 h. Even though this corresponds to a doubling of the overall product concentration compared to the experiments described above, the overall yield was disappointingly low. Moderate shaking was applied to maintain the suspension; hence, the enzyme may have undergone mechanical stress caused by the suspension. Or the surfactant properties of the reagents may have impaired the enzyme stability. Also, inhibitory effects of the elevated reagent concentrations cannot be excluded at present. Further studies are necessary to clarify the aspects of P450 peroxygenases stability and putative inactivation at elevated (co)-substrates concentrations and to establish a practical system for fatty acid hydroxylation.

2.5. Control experiments

Several control experiments were performed to detect the presence of possible background reactions. Thus, with respect to the standard enzyme-catalyzed reaction with full conversion (Fig. 5, column 1), the same reaction was carried out leaving out either BNAH or FMN or both (Fig. 5, columns 2–4). While the controls in the absence of BNAH were essentially negative, a small but significant product formation in the absence of FMN (as the H_2O_2-generation catalyst) was observed.

Principally, spontaneous aerobic oxidation of BNAH yielding H_2O_2 may account for this. However, control experiments on the stability of BNAH under the reaction conditions revealed that the rate of this autoxidation is too low to explain the background activity observed. At present, we also cannot fully exclude the presence of trace amounts of flavins (or other redox-active dyes originating from *E. coli*) to have remained in the enzyme preparations.

3. Conclusions

Overall, we demonstrated that the novel in situ H_2O_2 generation method presented here is a promising approach to promote P450 peroxygenases catalysis. Thus, the overall productivity could be enhanced due to higher enzyme operational stability at tailored H_2O_2 generation rates. Even though this work reports the proof-of-concept only, the most important parameters determining the efficiency to the overall system have been identified. The generation of H_2O_2 was the rate-limiting step, however it could be easily controlled via appropriate FMN and BNAH concentrations. Further characterization will result in an optimized ratio of FMN/BNAH/O_2/biocatalyst enabling high reaction rates while minimizing H_2O_2-related inactivation of the enzyme. Especially optimized aeration procedures are expected to fully exploit the preparative potential of this new approach.

So far, we have used BNAH in stoichiometric amounts. Envisaging preparative scale application of the in situ H_2O_2 generation method presented here we are going to evaluate recycling of the cofactor, as well as its in situ regeneration. For the latter approach, especially organometallic catalysts such as $[Cp^*Rh(bpy)H]^+$ coupling the reduction of BNA^+ to oxidation of formic acid, appear most promising.[4–6]

We believe that the novel in situ H_2O_2 system has a great potential and its future application can be extended to more biocatalytic systems.

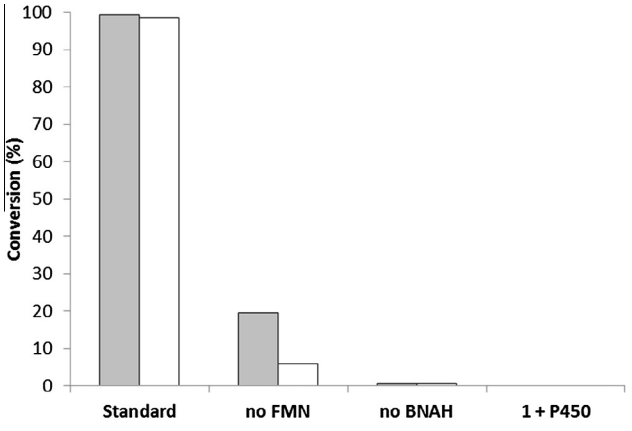

Figure 5. Product **2** and **3** formation with control reactions; $P450_{Cl\alpha}$ (grey), $P450_{Bs\beta}$ (white). Tris–HCl buffer (50 mM, pH 7.5), [myristic acid] = 200 μM, [FMN] = 60 μM, [BNAH] = 600 μM, [P450] = 1 μM (purified enzyme), 30 °C, 20 min.

4. Experimental

4.1. General details

All commercial reagents and solvents were purchased at the highest purity available and used as received. Cell-free extracts as well as purified $P450_{Cl\alpha}$ and $P450_{Bs\beta}$ were obtained as previously reported.[10] P450 concentrations of the enzyme preparations were determined by CO-difference spectral assay with $\varepsilon_{450-490}$ = 91 mM^{-1} cm^{-1}.[27] Catalase (2100 U/mg) from bovine liver was purchased from Sigma–Aldrich. Myristic acid, lauric acid, 2 hydroxymyristic acid, FMN, diethyl ether (Et_2O), hydrochloric acid (HCl), tris(hydroxymethyl)-aminomethane (Tris), ethyl acetate (EtOAc), dimethylsulfoxide, and *N*,*O*-bis(trimethylsilyl) trifluoroacetamide (BSTFA) containing trimethylchlorosilane (99:1) were purchased from Sigma–Aldrich in analytical pure grade and used as received. Melting points were taken on a Büchi melting point B-450 and are uncorrected. UV assays were performed on a Shimadzu UV–Vis spectrophotometer UV-2401 PC, with disposable plastic cuvettes of 1.5 mL in volume. NMR spectra were recorded on a Bruker Avance spectrometer at 300 (^1H) and 75 (^{13}C) MHz. GC-MS analyses were carried out on a Shimadzu GC-2010 apparatus coupled to a Shimadzu GCMS-QP2010S mass-selective detector with an AOC-20i auto-injector.

4.2. Synthesis

4.2.1. 1-Benzyl-3-carbamoylpyridinium bromide (BNA^+)

Following a previous procedure.[7] Nicotinamide (4.88 g, 40 mmol) was dissolved in acetonitrile (40 mL) and benzyl bromide (4.8 mL, 40 mmol) was added. The reaction mixture was refluxed for 15 h, after which time a precipitate was observed. The solution was cooled and Et_2O (50 mL) was added to further precipitate the final product. After filtering and washing with Et_2O (3 × 10 mL), the bromide salt 1-benzyl-3-carbamoylpyridium bromide BNA^+ was obtained as a white solid powder (10.9 g, 93%). Mp: 214–215 °C; the NMR data recorded corresponded to the previous procedure.[7]

4.2.2. 1-Benzyl-1,4-dihydronicotinamide (BNAH)

Following a previous procedure.[7] Under nitrogen atmosphere, 1-benzyl-3-carbamoylpyridinium bromide BNA^+ (2.93 g, 10 mmol) was dissolved in distilled H_2O (60 mL) and $NaHCO_3$ (4.20 g, 50 mmol) was added. Sodium dithionite $Na_2S_2O_4$ (8.71 g, 50 mmol) was then added in small portions and the reaction mixture was stirred at room temperature for 3 h in the dark, during which time the solution turned from orange to yellow as the yellow product precipitated. The solid was filtered, washed with ice-cold H_2O (3 × 10 mL) and dried over phosphorus pentoxide (P_2O_5) under reduced pressure to afford product 1-benzyl-1,4-dihydronicotinamide BNAH as a bright yellow powder (1.71 g, 80%). Mp: 111–114 °C; the NMR data recorded corresponded to the previous procedure.[7]

4.3. Enzyme-catalyzed reaction conditions

The following buffers and stock solutions were used: Tris–HCl buffer (50 mM, pH 7.5), FMN (1 mM aqueous solution), myristic acid (20 mM in DMSO), lauric acid (20 mM in DMSO). Fresh stock solution of BNAH (10–100 mM) was prepared in methanol before each use.

The reactions were performed in microcentrifuge plastic tubes (2 mL in volume) at 30 °C, under ambient atmosphere, unless otherwise mentioned. The reaction mixture contained Tris–HCl buffer (50 mM, pH 7.5; final volume of 1 mL), myristic acid (200 μM), FMN (40–250 μM), BNAH (200–600 μM), $P450_{Cl\alpha}$ (1 μM) or $P450_{Bs\beta}$ (1 μM), DMSO (1% v/v), MeOH (1% v/v). The reaction assays were mixed at 1200 rpm for 5–20 min depending on the experiment. The reaction was stopped at the indicated time intervals through the addition of concentrated HCl (40 μL, 37% w/w) followed by addition of lauric acid (10 μL) as an external standard. The reaction mixtures were extracted twice with 1 mL Et_2O. After evaporation of the Et_2O, the remaining reagents were dissolved in BSTFA (200 μL) and incubated in a thermoshaker for 30 min at 80 °C and 1200 rpm. After cooling down to room temperature the samples were transferred to the glass GC vials and analyzed by GC or GC-MS. All control experiment were performed identically excluding one of the reaction components. To confirm the peroxygenase activity standard reaction assay was performed upon addition of catalase from bovine liver (2100 U/mg).

The semi-preparative scale was performed with the following reaction conditions: Tris–HCl buffer (50 mM, pH 7.5), [myristic acid] = 10 mM, [FMN] = 60 μM, $[P450_{Cl\alpha}]$ = 1 μM, [BNAH] = 50 mM, at 30 °C during 70 h.

4.4. GC analysis

The progress of the reaction was followed using gas chromatography (GC) and the final product concentrations were calculated based on calibration curve equations using an external standard (lauric acid). GC-MS analysis was performed with He as carrier gas and a Varian FactorFour VF-1ms column (25 m × 0.25 mm × 0.4 μm). Column oven program: 50 °C, 60 °C/min to 212 °C, 8 min, 60 °C/min to 325 °C, 5 min; linear velocity: 37 cm/s; split ratio: 5. Characteristic mass fragmentation patterns were obtained from the EI-MS using ion source (200 °C); scan mode with an m/z range 40–600 in 0.5 s.

Myristic acid (retention time t_R 5.54 min), lauric acid (t_R 4.25 min) and 2-hydroxymyristic acid (t_R 7.45 min) were also assigned using authentic standards. The peak of 3-hydroxymyristic acid at 7.69 min was identified by the mass fragmentation pattern in the GC-MS chromatogram. The regioselectivity for α:β hydroxylation were 1:1.7 for $P450_{Bs\beta}$ and 24:1 for $P450_{Cl\alpha}$.

4.5. UV spectrophotometry

The depletion rate of BNAH was determined with a UV–Vis spectrophotometer following the decrease of the characteristic UV absorbance of BNAH at 360 nm. The experiments were performed in disposable plastic UV cuvettes (1.5 mL in volume) at 30 °C with Tris–HCl buffer (50 mM pH 7.5), on a Shimadzu UV-2401 PC spectrophotometer with a Julabo F12 Refrigerated/Heating Circulator. The stock solution of BNAH was diluted in buffer to final concentration of 10–400 μM, and the samples were incubated for 5 min at 30 °C. The reactions were initiated by the addition of the FMN solution to a final concentration of 10–250 μM. All experiments were performed in triplicates obtaining a standard deviation below 15%.

4.6. Oxygen Clark electrode

Oxygen consumption was measured on Strathkelvin 782 2-Channel oxygen system using Strathkelvin 1302 Clark-type microcathode oxygen electrodes. The measurements were done in a water-jacketed respiration chamber made from precision bore glass covered by aluminium foil to prevent flavin illumination by light; the water-jacket was connected to a thermally controlled water system at 25 °C. The chamber was placed on a magnetic stirrer. The electrode was calibrated prior to measurements.

The following buffers and concentrations were used: phosphate buffer KPi (50 mM, pH 7.0), BNAH (100 μM), FMN (10–250 μM). The buffer was saturated with oxygen prior to usage. The reactions were initiated by the addition of FMN and the electrode holder was immersed into the chamber immediately. Oxygen consumption was followed by the decrease in oxygen concentration using the Strathkelvin software. All experiments were performed in triplicates obtaining a standard deviation below 15%. The oxygen consumption rate correlated with the BNAH depletion rate (Fig. 1).

Acknowledgments

This work was supported by the Marie Curie IEF 'BIOTRAINS' and 'BIOMIMIC' financed by the European Union through the 7th Framework People Programme (Grant agreement number 238531 and 327647). Maarten Gorseling (Delft University of Technology) and Melanie Wachtmeister (Heinrich-Heine University Düsseldorf) are gratefully acknowledged for their technical assistance.

References and notes

1. Paul, C. E.; Arends, I. W. C. E.; Hollmann, F. *ACS Catal.* **2014**, *4*, 788.
2. Sicsic, S.; Durand, P.; Langrene, S.; Goffic, F. L. E. *Eur. J. Biochem.* **1986**, *155*, 403.
3. Sicsic, S.; Durand, P.; Langrene, S.; Legoffic, F. *FEBS Lett.* **1984**, *176*, 321.
4. Lo, H. C.; Fish, R. H. *Angew. Chem., Int. Ed.* **2002**, *41*, 478.
5. Ryan, J. D.; Fish, R. H.; Clark, D. S. *ChemBioChem* **2008**, *9*, 2579.
6. Lutz, J.; Hollmann, F.; Ho, T. V.; Schnyder, A.; Fish, R. H.; Schmid, A. *J. Organomet. Chem.* **2004**, *689*, 4783.
7. Paul, C. E.; Gargiulo, S.; Opperman, D. J.; Lavandera, I.; Gotor-Fernandez, V.; Gotor, V.; Taglieber, A.; Arends, I. W. C. E.; Hollmann, F. *Org. Lett.* **2013**, *15*, 180.
8. Massey, V. *J. Biol. Chem.* **1994**, *269*, 22459.
9. Matsunaga, I.; Ueda, A.; Fujiwara, N.; Sumimoto, T.; Ichihara, K. *Lipids* **1999**, *34*, 841.
10. Girhard, M.; Schuster, S.; Dietrich, M.; Dürre, P.; Urlacher, V. B. *Biochem. Biophys. Res. Commun.* **2007**, *362*, 114.
11. Girhard, M.; Kunigk, E.; Tihovsky, S.; Shumyantseva, V. V.; Urlacher, V. B. *Biotechnol. Appl. Biochem.* **2013**, *60*, 111.
12. Matsunaga, I.; Yamada, M.; Kusunose, E.; Nishiuchi, Y.; Yano, I.; Ichihara, K. *FEBS Lett.* **1996**, *386*, 252.
13. Urlacher, V. B.; Girhard, M. *Trends Biotechnol.* **2012**, *30*, 26.
14. Urlacher, V. B.; Eiben, S. *Trends Biotechnol.* **2006**, *24*, 324.
15. Urlacher, V.; Schmid, R. D. *Curr. Opin. Biotechnol.* **2002**, *13*, 557.
16. Valderrama, B.; Ayala, M.; Vazquez-Duhalt, R. *Chem. Biol.* **2002**, *9*, 555.
17. van Deurzen, M. P. J.; van Rantwijk, F.; Sheldon, R. A. *Tetrahedron* **1997**, *53*, 13183.
18. Karmee, S. K.; Roosen, C.; Kohlmann, C.; Lütz, S.; Greiner, L.; Leitner, W. *Green Chem.* **2009**, *11*, 1052.
19. Lutz, S.; Vuorilehto, K.; Liese, A. *Biotechnol. Bioeng.* **2007**, *98*, 525.
20. La Rotta Hernandez, C. E.; Lütz, S.; Liese, A.; Bon, E. P. S. *Enzyme Microb. Technol.* **2005**, *37*, 582.
21. Getrey, L.; Krieg, T.; Hollmann, F.; Schrader, J.; Holtmann, D. *Green Chem.* **2014**, *16*, 1104.
22. Krieg, T.; Huttmann, S.; Mangold, K.-M.; Schrader, J.; Holtmann, D. *Green Chem.* **2011**, *13*, 2686.
23. Churakova, E.; Arends, I. W. C. E.; Hollmann, F. *ChemCatChem* **2013**, *5*, 565.
24. Churakova, E.; Kluge, M.; Ullrich, R.; Arends, I.; Hofrichter, M.; Hollmann, F. *Angew. Chem., Int. Ed.* **2011**, *50*, 10716.
25. Perez, D. I.; Mifsud Grau, M.; Arends, I. W. C. E.; Hollmann, F. *Chem. Commun.* **2009**, 6848.
26. Honda Malca, S.; Girhard, M.; Schuster, S.; Dürre, P.; Urlacher, V. B. *Biochimica et Biophysica Acta (BBA)—Proteins Proteomics* **2011**, *1814*, 257.
27. Omura, T.; Sato, R. *J. Biol. Chem.* **1964**, *239*, 2370.